SUPPLEMENTARY INFORMATION

SUPPLEMENTARY MATERIALS AND METHODS

Cloning of retroviral and non-viral expression plasmids

To improve expression levels of SB100X and FLP, we used codon-optimized variants, termed SB100Xo and FLPo. Using gene synthesis (GeneArt, Regensburg, Germany), the SB100X codons were adapted to optimal tRNA usage codons for *Homo sapiens* and cryptic splice and polyadenylation sites as well as mRNA secondary structures were removed to increase mRNA stability and translatability. Likewise, we took advantage of a codon-optimized variant of FLP named FLPo (1) (kindly provided by P. Soriano, Seattle, WA). To facilitate cloning we introduced restriction sites AgeI, SalI and EcoRI flanking SB100Xo or AgeI and SalI flanking FLPo.

Lentiviral and gammaretroviral bidirectional FLPo, SB100X and SB100Xo vectors were derived from LBid.EGFP.SF.mCherry.PRE* and RBid.EGFP.SF.mCherry.PRE* (2). Replacing the mCherry cDNA of the latter by either SB100Xo or FLPo as AgeI / SalI fragments resulted in LBid.EGFP.SF.SB100Xo.PRE*, RBid.EGFP.SF.SB100Xo.PRE*, LBid.EGFP.SF.FLPo.PRE* and RBid.EGFP.SF.FLPo.PRE*, respectively. For generation of LBid.EGFP.SF.SB100X.PRE* and RBid.EGFP.SF.SB100X.PRE* a blunted SB100X fragment (ApaI / SpeI) derived from pCMV.SB100X (3) was exchanged against mCherry within the corresponding bidirectional vectors via blunted AgeI / SalI sites.

All gammaretroviral iRV and RMT variants were based on SF91.EGFP (4,5) or SF91aPBS.EGFP (6). SF91.FLPo and SF91aPBS.FLPo were generated by introducing FLPo (AgeI / EcoRI) derived from RBid.EGFP.SF.FLPo.PRE* into SF91.EGFP or SF91aPBS.EGFP (both AgeI / EcoRI). RSF91.FLPo resulted from ligation of FLPo (AgeI / EcoRI) derived from RBid.EGFP.SF.FLPo.PRE* (2) into RSF91.EGFP.PRE (AgeI / EcoRI; (7,8)). Exchanging the backbone of RSF91.FLPo against the aPBS-containing backbone of RSF91aPBS.SB100Xo (see below) via an ApaI / NheI digest resulted in RSF91aPBS.FLPo. Finally, the PRE element (900 bp) excised from RSF91.EGFP.PRE via EcoRI was inserted into linearized RSF91.FLPo (EcoRI) resulting in RSF91.FLPo.PRE. Again, introduction of the aPBS was carried out by ligating the FLPo.PRE expression cassette from RSF91.FLPo.PRE as ApaI / NheI fragment into the RSF91.aPBS backbone (ApaI / NheI) of RSF91aPBS.SB100Xo.

To generate SF91aPBS.cSB, the conventional SB10 transposase was introduced as NotI / EcoRI fragment from pFVA.SB10 (9) into SF91aPBS.EGFP. SF91aPBS.SB100X was cloned by inserting SB100X as a blunted fragment (ApaI / SpeI) derived from pCMV.SB100X into the blunted SF91aPBS.EGFP vector linearized with AgeI / EcoRI. An AgeI and EcoRI digest was used to replace the EGFP of SF91aPBS.EGFP by the synthesized SB100Xo.

Introduction of the RSV promoter was carried out by cloning the SB containing NotI / XhoI fragment of SF91aPBS.cSB or SF91aPBS.SB100X or SF91aPBS.SB100Xo into the likewise digested RSF91aPBS.nlsCre (8) backbone. The 900 bp PRE fragment from Woodchuck Hepatitis Virus (7,10) was inserted into linearized RSF91aPBS.cSB as an EcoRI fragment derived from RSF91.FLPo.PRE. RSF91aPBS.SB100X.PRE resulted from introducing a blunted version of the same PRE fragment (EcoRI) into linearized and blunted RSF91aPBS.SB100X (BamHI). Replacement of FLPo in RSF91aPBS.FLPo.PRE by SB100Xo (AgeI / SalI) led to generation of RSF91aPBS.SB100Xo.PRE. Integrating RSF91.cSB.PRE, RSF91.SB100X.PRE and RSF91.SB100Xo.PRE vectors are constructed in the same way as their RT-deficient aPBS counterparts.

To inhibit the catalytic activity of SB100X all three residues of the corresponding DDE motif were mutated (11,12). Inactivation was performed by first replacing the glutamic acid residue (E) by alanine (A). This single point mutation was introduced via overlapping PCR into RSF91.SB100X.PRE using primer pairs 5'-GACCTCAATCCTATA**GCC**AATTTGTGGGCAG-3' and 5'-TTGATCCGAATTCCTAGTATTTGG-3' as well as 5'-CACAAATT**GGC**TATAGGATTGAGGTCAGGG-3' and 5'-GTTGTGGCAAAATGGCTTAAGG-3'. The resulting PCR fragment was subcloned, sequenced and cloned into RSF91.SB100X.PRE via 3-fragment-ligation (using enzymes AflII, EcoRI and NotI) generating RSF91.SB100XmutE/A.PRE. Mutation of the remaining aspartic acid residues (DD→AA) were carried out by a second round of overlapping PCR using primer pairs 5'-TCCTCTGGTCT**GCC**GAAACAAAAATAGAACTG-3' and 5'-TTGTCCTTAAGCCATTTTGCCACAACTTTGGAAGTATGCTTGGGGTCATT**GGC**GTGTTG G-3' as well as 5'-TATTTTTGTTTC**GGC**AGACCAGAGGACATTTCTCC-3' and 5'-TCAGGAAGGAGACGCGTTCTG-3' and RSF91.SB100XmutE/A.PRE as a template. The resulting PCR fragment was also subcloned, sequenced and introduced into RSF91.SB100XmutE/A.PRE via 3-fragment ligation using enzymes MluI, AflII and EcoRI. The resulting vector was named RSF91.SB100XtripleMut.PRE or iRV.mutSB100X for simplicity. Restriction sites within primers that were used for cloning are underlined and the mutated codons are shown in bold.

To construct a lentiviral SIN vector harboring a transposable element (pRRL.PPT.IR/DR.SF.EGFP.pA), we included the 5' and 3' Sleeping Beauty inverted and directed repeats (IR/DR) flanking an EGFP expression cassette driven by the SFFV promoter and terminated by the SV40 pA into a lentiviral vector. In more detail, the 5' IR/DR was amplified using 5' 5IR nhe 5'-GAGCTAGCCTACAGTTGAAGTCGGAAGTTTAC-3' and 3' 5IR nhe 5'-CAGCTAGCTTGAAATACATCCACAGGTACACC-3' primers (restriction sites are underlined) using pT-Zeo (13) as a template and the resulting NheI fragment was introduced into the lentiviral SIN vector pRRL.PPT.SF.EGFPpre (14). Likewise, the 3' IR/DR were

amplified using primers 5' 3IR bsrgi eco47iii 5'-GCTGTACAAGTGATAGCGCTCCCATCACAAAGCTCTGACCTCA-3' and 3' 3IR acc65i 5'-AAGGTACCTACAGTTGAAGTCGGAAGTTTACA-3' and introduced as a BsrGI / Acc65I fragment into the above mentioned lentiviral SIN vector. To introduce a polyA signal into the transposable element, the SV40pA was amplified from pEGFP-N1 (Clontech, Heidelberg, Germany) using primers 5' SV40pA eco47iii ecori 5'-ATAGCGCTGAATTCAACTTGTTTATTGCAGCTTATAAT-3' and 3' SV40pA eco47iii 5'-GGAGCGCTAAGATACATTGATGAGTTTGGACA-3' and included into the previously generated Eco47III site.

Using DNA synthesis (MrGene, Regensburg, Germany) we generated an improved version of the transposable element including 5'IR/DR and 3'IR/DR as well as multiple unique restriction sites (Acc65I, RsrII, NheI, AgeI, AvaI, XhoI, NotI, BglII, BamHI, SnaBI, SalI, EcoRI, EcoRV, AflIII) to facilitate modular exchange of individual components. First, the synthesized transposable element was cloned via *an* Acc65I / AflII fragment into pSK-II+ (Stratagene, Heidelberg, Germany) to generate pSK.IR Next, the SV40pA was amplified (15) and inserted via BamHI / BglII into pSK.IR. To accomplish pSK.IR.SF.EGFP.pA.IR the SFFV-EGFP cassette of SERS11.SF.EGFP.PRE* (8) was excised and cloned via a NotI / NheI fragment into pSK.IR.pA. The transposable element pSK.IR.SF.mCherry.pA.IR was generated by replacing EGFP by mCherry (AgeI / NotI) (16) derived from pRBid.nlsCre.SF.mCherry.PRE* (2). All PCR products were fully sequenced. Further vector details are available upon request.

RMT vector titration

Retroviral RSF91.EGFP.PRE (iRV.EGFP), RSF91aPBS.cSB.PRE (RMT.cSB), RSF91aPBS.SB100X.PRE (RMT.SB100X) and RSF91aPBS.SB100Xo.PRE (RMT.SB100Xo) supernatants were identically produced, harvested and concentrated over night via ultracentrifugation at 13,000 x g and 4℃ . The retroviral pellets were resuspended in ice cold phosphate-buffered saline, aliquotted and stored at -80℃ until usage. For RNA content determination, supernatants were extensively pretreated with RNase-free Turbo DNAse (Ambion / Applied Biosystems, Darmstadt, Germany), and the retroviral RNA was extracted by using RNeasy Micro kit columns (Quiagen, Hilden, Germany) according to the manufacturer's protocol, including an additional DNase treatment. First strand synthesis and quantitative PCR for detection of the vector encoded PRE element was carried out as previously described (17) and as mentioned in the main manuscript, respectively. A plasmid containing the PRE sequence served as standard for the quantification of retroviral vector copy numbers (18). All samples were checked for remaining plasmid contamination and retroviral gRNA copy numbers were corrected accordingly.

Retroviral episomal transfer of Sleeping Beauty transposase

Analogous to the RMT based SB assay, 2 x 10^5 HeLa cells were seeded and transduced the following day with serial dilutions of integrase defective lentiviral or gammaretroviral bidirectional vector particles. Twenty-two hours later transduced cells were transfected (PEI) with 600 ng pSK.IR.SF.mCherry.pA.IR encoding for the red fluorescent mCherry protein (16). The percentage of EGFP and mCherry double positive cells were determined via flow cytometry 2 and 14 days post transfection and the values were used for the calculation of the transposition rates. Cells being just transfected with pSK.IR.SF.mCherry.pA.IR served as control.

Retroviral transduction of CF1 murine embryonic fibroblasts

CF1 MEFs were purchased from (GlobalStem, Rockville, Maryland, USA) and cultured in DMEM low glucose medium supplemented with 10% FCS, 1% Penicillin / Streptomycin, 1% glutamine, 1% non-essential amino acids and 100 pM β-mercaptoethanol. For transduction 5 x 10^4 cells were seeded into gelatine (0.1% in PBS) coated wells of a 12-well-plate. The next day cells were either transduced with 50 µl of concentrated iRV SB vector particles (RSF91+PRE) or cotransduced with concentrated RMT.SB100Xo (150 µl) and eLVTE (50 µl) vector particles encoding for EGFP. Cells were measured by flow cytometry and stained with AnnexinV for apoptotic cells at the indicated time points. Successful transposition was also confirmed by quantitative real-time PCR using primers 5'-CTATATCATGGCCGACAAGCAGA-3' and 5'-GGACTGGGTGCTCAGGTAGTGG-3' detecting EGFP (19). Data were normalized to the signal obtained from the amplification of murine FLK1 intron enhancer sequences with primers 5'-GGTTTCAATGTCCCGTATCCTT-3' and 5'-CTTTGCCCCAGTCCCAGTTA-3' (20) and quantified using the comparative threshold cycle method.

Cytotoxicity assay of transfected SB transposase expression plasmids

Four hundred thousand HeLa cells were cotransfected with 600 ng pSK.IR.SF.EGFP.pA.IR (TE) and increasing amounts (10 ng , 50 ng , 100 ng , 250 ng , 500 ng and 1000 ng) of gammaretroviral and nonviral transposase expression plasmids (pRSF91aPBS.cSB.PRE, pRSF91aPBS.SB100X.PRE, pRSF91aPBS.SB100Xo.PRE and pCMV.SB100X) using the PEI transfection reagent. Differences in plasmid quantity were adjusted with pUC19 DNA, resulting in 1600 ng transfected plasmid DNA per well. Two micrograms of gammaretroviral pSF91aPBS.EGFP.PRE (pRMT.EGFP, (17)) served as control for the gammaretroviral vector backbone expression unit. Four days post transfection cells were harvested and analyzed via trypan blue and AnnexinV staining for dead and apoptotic cells, respectively.

SUPPLEMENTARY REFERENCES

1. Raymond, C.S. and Soriano, P. (2007) High-efficiency FLP and PhiC31 site-specific recombination in mammalian cells. *PLoS One*, **2**, e162.
2. Maetzig, T., Galla, M., Brugman, M.H., Loew, R., Baum, C. and Schambach, A. (2010) Mechanisms controlling titer and expression of bidirectional lentiviral and gammaretroviral vectors. *Gene Ther*, **17**, 400-411.
3. Mates, L., Chuah, M.K., Belay, E., Jerchow, B., Manoj, N., Acosta-Sanchez, A., Grzela, D.P., Schmitt, A., Becker, K., Matrai, J. *et al.* (2009) Molecular evolution of a novel hyperactive Sleeping Beauty transposase enables robust stable gene transfer in vertebrates. *Nat Genet*, **41**, 753-761.
4. Hildinger, M., Abel, K.L., Ostertag, W. and Baum, C. (1999) Design of 5' untranslated sequences in retroviral vectors developed for medical use. *J Virol*, **73**, 4083-4089.
5. Schambach, A., Wodrich, H., Hildinger, M., Bohne, J., Krausslich, H.G. and Baum, C. (2000) Context dependence of different modules for posttranscriptional enhancement of gene expression from retroviral vectors. *Mol Ther*, **2**, 435-445.
6. Galla, M., Will, E., Kraunus, J., Chen, L. and Baum, C. (2004) Retroviral pseudotransduction for targeted cell manipulation. *Mol Cell*, **16**, 309-315.
7. Schambach, A., Bohne, J., Baum, C., Hermann, F.G., Egerer, L., von Laer, D. and Giroglou, T. (2006) Woodchuck hepatitis virus post-transcriptional regulatory element deleted from X protein and promoter sequences enhances retroviral vector titer and expression. *Gene Ther*, **13**, 641-645.
8. Schambach, A., Mueller, D., Galla, M., Verstegen, M.M., Wagemaker, G., Loew, R., Baum, C. and Bohne, J. (2006) Overcoming promoter competition in packaging cells improves production of self-inactivating retroviral vectors. *Gene Ther*, **13**, 1524-1533.
9. Ivics, Z., Hackett, P.B., Plasterk, R.H. and Izsvak, Z. (1997) Molecular reconstruction of Sleeping Beauty, a Tc1-like transposon from fish, and its transposition in human cells. *Cell*, **91**, 501-510.
10. Hope, T. (2002) Improving the post-transcriptional aspects of lentiviral vectors. *Curr Top Microbiol Immunol*, **261**, 179-189.
11. Plasterk, R.H., Izsvak, Z. and Ivics, Z. (1999) Resident aliens: the Tc1/mariner superfamily of transposable elements. *Trends Genet*, **15**, 326-332.
12. Belay, E., Matrai, J., Acosta-Sanchez, A., Ma, L., Quattrocelli, M., Mates, L., Sancho-Bru, P., Geraerts, M., Yang, B., Joris, V. *et al.* (2010) Novel Hyperactive Transposons for Genetic Modification of Induced Puripotent and Adult Stem Cells: A Non-Viral Paradigm for Coaxed Differentiation. *Stem Cells.*
13. Vigdal, T.J., Kaufman, C.D., Izsvak, Z., Voytas, D.F. and Ivics, Z. (2002) Common physical properties of DNA affecting target site selection of sleeping beauty and other Tc1/mariner transposable elements. *J Mol Biol*, **323**, 441-452.
14. Schambach, A., Galla, M., Modlich, U., Will, E., Chandra, S., Reeves, L., Colbert, M., Williams, D.A., von Kalle, C. and Baum, C. (2006) Lentiviral vectors pseudotyped with murine ecotropic envelope: Increased biosafety and convenience in preclinical research. *Exp Hematol*, **34**, 588-592.
15. Loew, R., Vigna, E., Lindemann, D., Naldini, L. and Bujard, H. (2006) Retroviral vectors containing Tet-controlled bidirectional transcription units for simultaneous regulation of two gene activities. *J Mol Genet Med*, **2**, 107-118.
16. Shaner, N.C., Campbell, R.E., Steinbach, P.A., Giepmans, B.N., Palmer, A.E. and Tsien, R.Y. (2004) Improved monomeric red, orange and yellow fluorescent proteins derived from Discosoma sp. red fluorescent protein. *Nat Biotechnol*, **22**, 1567-1572.
17. Galla, M., Schambach, A., Towers, G.J. and Baum, C. (2008) Cellular restriction of retrovirus particle-mediated mRNA transfer. *J Virol*, **82**, 3069-3077.
18. Heinz, N., Schambach, A., Galla, M., Maetzig, T., Baum, C., Loew, R. and Schiedlmeier, B. (2010) Retroviral and transposon-based tet-regulated All-In-One vectors with reduced background expression and improved dynamic range. *Hum Gene Ther*.
19. Schambach, A., Galla, M., Maetzig, T., Loew, R. and Baum, C. (2007) Improving Transcriptional Termination of Self-inactivating Gamma-retroviral and Lentiviral Vectors. *Mol Ther*, **15**, 1167-1173.
20. Wicke, D.C., Meyer, J., Buesche, G., Heckl, D., Kreipe, H., Li, Z., Welte, K.H., Ballmaier, M., Baum, C. and Modlich, U. (2010) Gene therapy of MPL deficiency: challenging balance between leukemia and pancytopenia. *Mol Ther*, **18**, 343-352.

Galla et al. 2011

Supplementary Figure S1

Supplementary Figure S1. Alignment of the SB100X and SB100Xo cDNAs. To achieve better SB100X expression, the SB100X cDNA was adapted to optimal tRNA usage for Homo sapiens. Furthermore, cryptic splice and polyadenylation sites as well as extensive RNA secondary structures were avoided. Sequence homology of SB100X and codon-optimized SB100Xo cDNAs was 75%, the resulting amino acid sequence was not altered. Identical nucleotides are highlited in blue.

Galla et al. 2011

Supplementary Figure S2

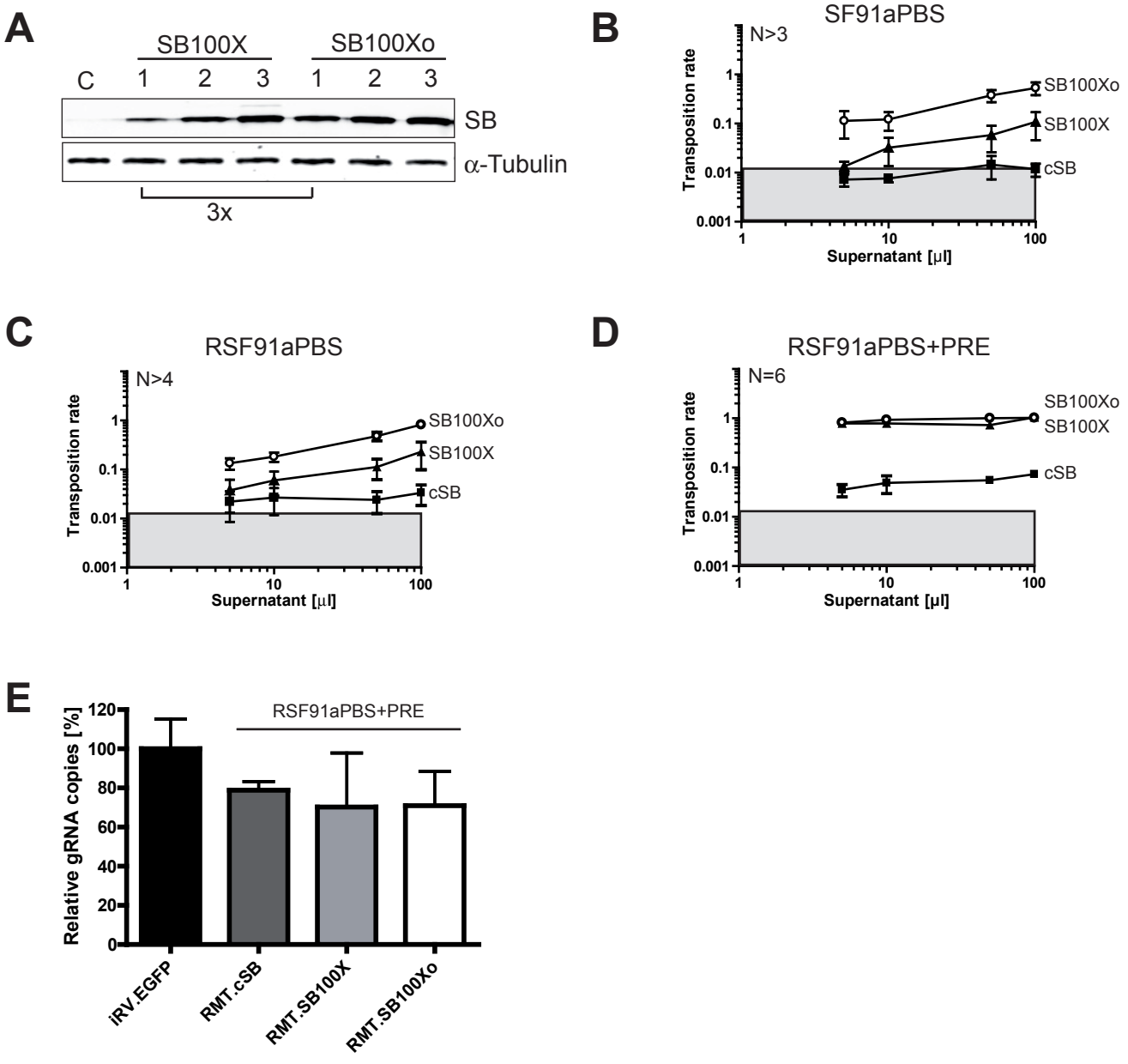

Supplementary Figure S2. Improved vector design leads to efficient SB transposition in HeLa cells. (**A**) At least threefold enhanced SB100X protein expression levels due to codon-optimization. 293T cells were equally transfected with either pSF91aPBS (1), pRSF91aPBS (2) or pRSF91aPBS +PRE (3) each encoding for SB100X or SB100Xo and analyzed for SB transposase expression levels by western blot analysis. α-Tubulin served as loading control. (**B**)–(**D**) Transposition rates in relation to the 3 vector backbones (see also Figure 1E and F) and the respective 3 SB transposase variants. RMT mediated transposition rates increase with better functionality/expression of the SB transposase (SB100Xo > SB100X > cSB) and depending on enhanced vector architecture (RSF91+PRE > RSF91 > SF91). The light gray shaded areas reflect the mean background plasmid integration levels (transposable element) of all experiments shown. (**E**) Comparable relative genomic RNA copy numbers among RMT supernatants. Retroviral RMT particles as used in (D) were produced, concentrated and 3x DNase digested. The retroviral RNA genomes were reverse transcribed and quantified using Real-Time PCR. All samples were checked for remaining plasmid contamination (<0.02% of sample values) and retroviral gRNA copy numbers were corrected accordingly. The graph depicts relative copy numbers of RMT genomes in comparison to a corresponding integrating EGFP vector (RSF91+PRE). Two independent experiments are shown.

Galla et al. 2011
Supplementary Figure S3

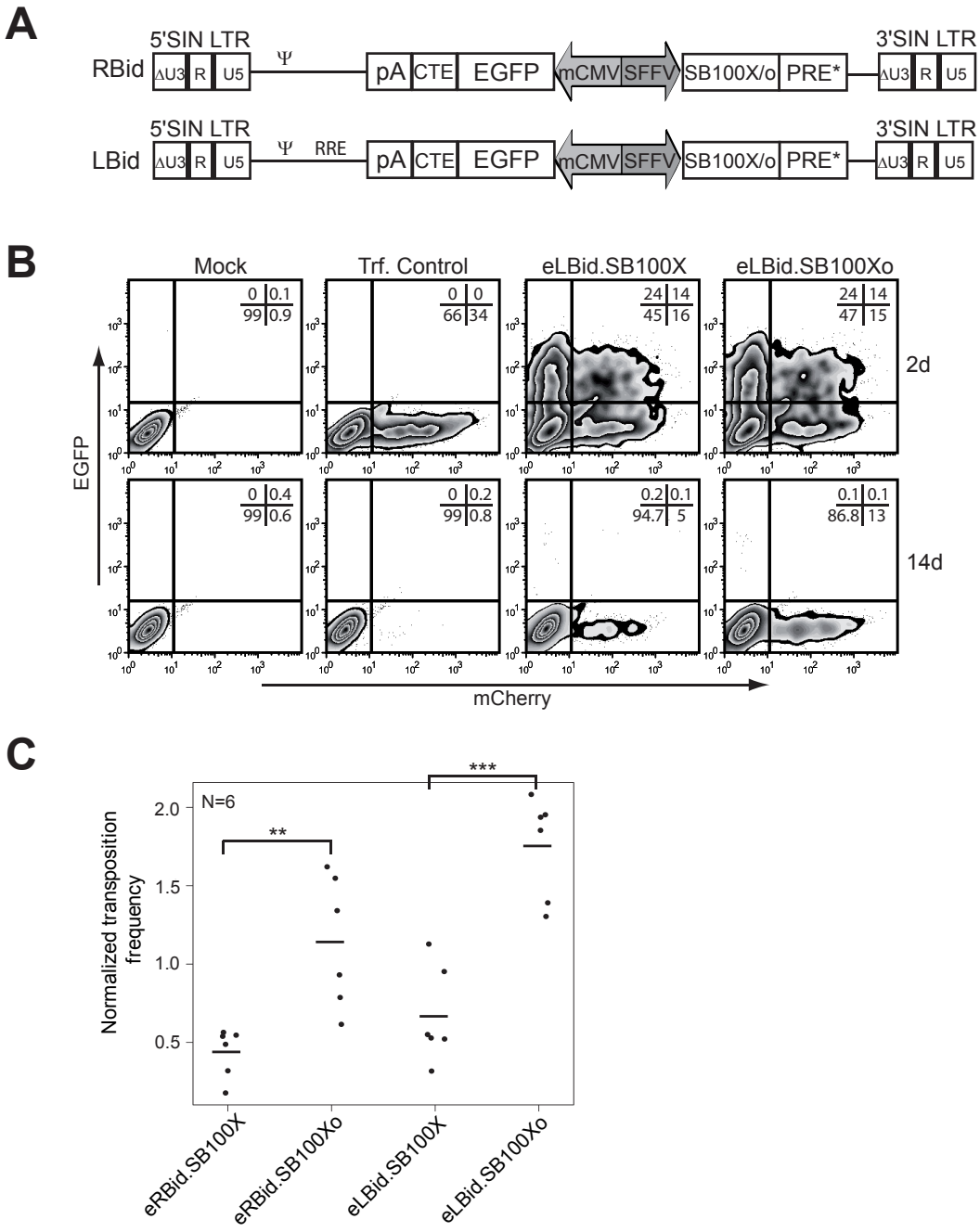

Supplementary Figure S3. Enhanced transposition frequency from episomal gammaretro- (RBid) and lentiviral (LBid) bidirectional vectors encoding for SB100Xo. (**A**) Schematic diagram of the used bidirectional vector self-inactivating (SIN) backbones (see also (2)). In brief, a bidirectional promoter drives a SB100X or SB100Xo (SB100X/o) expression cassette in sense and in antisense an EGFP cassette. pA: polyA signal; CTE: Mason-Pfizer Monkey Virus constitutive transport element; PRE*: 600 bp posttranscriptional regulatory element, devoid of the X ORF (7); Ψ: Packaging signal; RRE: Rev responsive element. (**B**) Enhanced transposition in HeLa cells transduced with episomal LBid.SB100Xo. First, cells were transduced with either episomal LBid.SB100X or LBid.SB100Xo particles and after 22 h transfected with a transposable element harboring a mCherry expression cassette (see also Figure 1C). Two and 14 days post transfection, cells were analyzed for EGFP and mCherry expression. Remaining mCherry expression at day 14 indicated successful transposition. (**C**) Summary of 6 independent experiments (n=6) of equally transduced and transfected cells (measured 2 days post transfection) for episomal RBid and LBid vector expressing either SB100X or SB100Xo. Data were normalized by the maximum value (highest transposition rate) for each data set. Statistics and P-values (eRBid.SB100X versus eRBid.SB100Xo: $P<0.01$; eLBid.SB100X versus eLBid.SB100Xo: $P<0.001$) were calculated by the Wilcoxon test.

Galla et al. 2011

Supplementary Figure S4

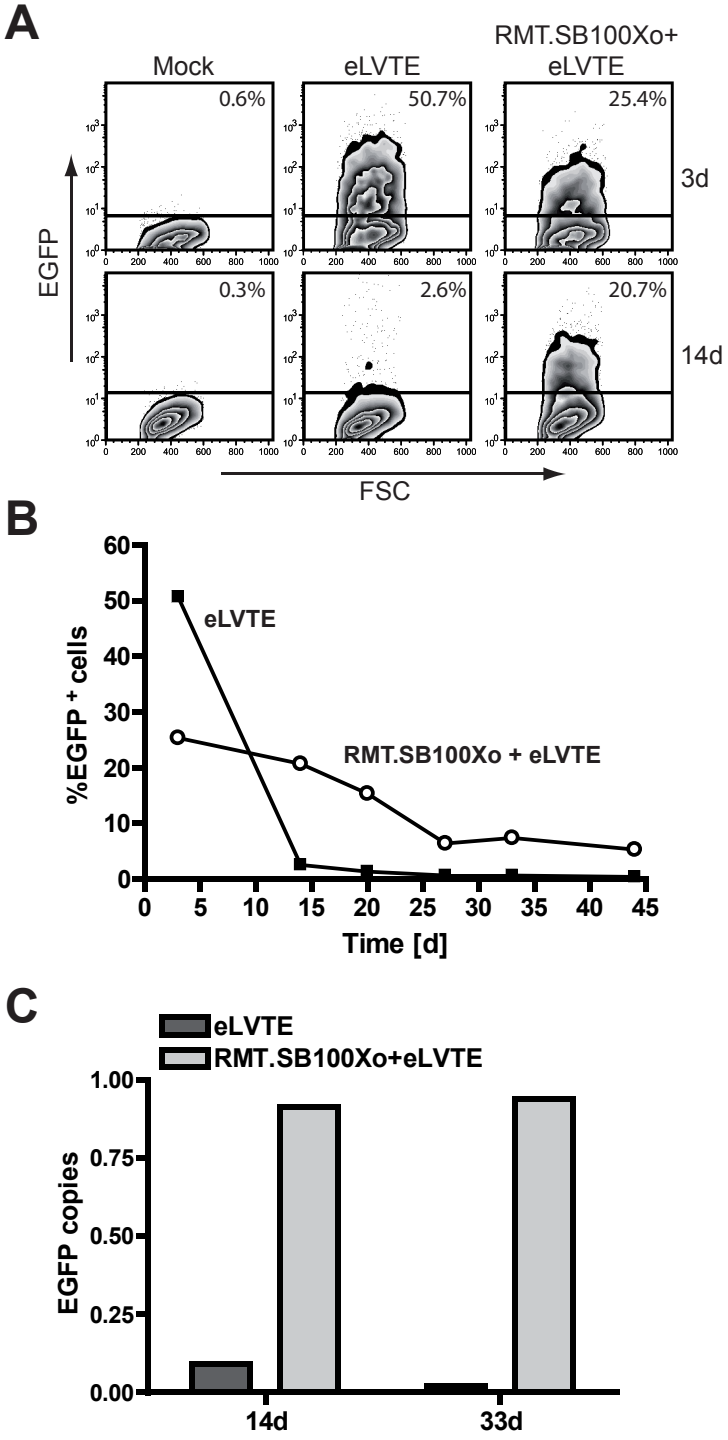

Supplementary Figure S4. Highly efficient transposition into murine embryonic fibroblasts (MEFs) via RMT. (**A**)-(**C**) CF1 MEFs were cotransduced with 150 µl concentrated RMT.SB100Xo (RSF91+PRE) and 50 µl concentrated eLVTE (MOI ~70) particles encoding for EGFP. Resulting EGFP expression was monitored over time by flow cytometry at the indicated time points. Strikingly, 14 d post transduction a transposition frequency of ~80% was observed (A). However, continuative kinetics of the transposed cell population revealed that EGFP protein expression levels declined over time (B). In contrast, the proportion of integrated EGFP DNA copies (transposable element) remained stable over time (C) arguing that the loss of EGFP expression is due to silencing of the SFFV promoter/enhancer regions rather than loss of the transposable element. Genomic DNA of CF1 MEFs either transduced with RMT.SB100Xo and eLVTE or only with eLVTE particles was analyzed via quantitative PCR for transposable element copy numbers 14 and 33 days post transduction. Primers were directed against the EGFP cDNA (17) and obtained Ct values were normalized to polypyrimidine tract-binding protein 2 (PTB2) (20) levels.

Galla et al. 2011

Supplementary Figure S5

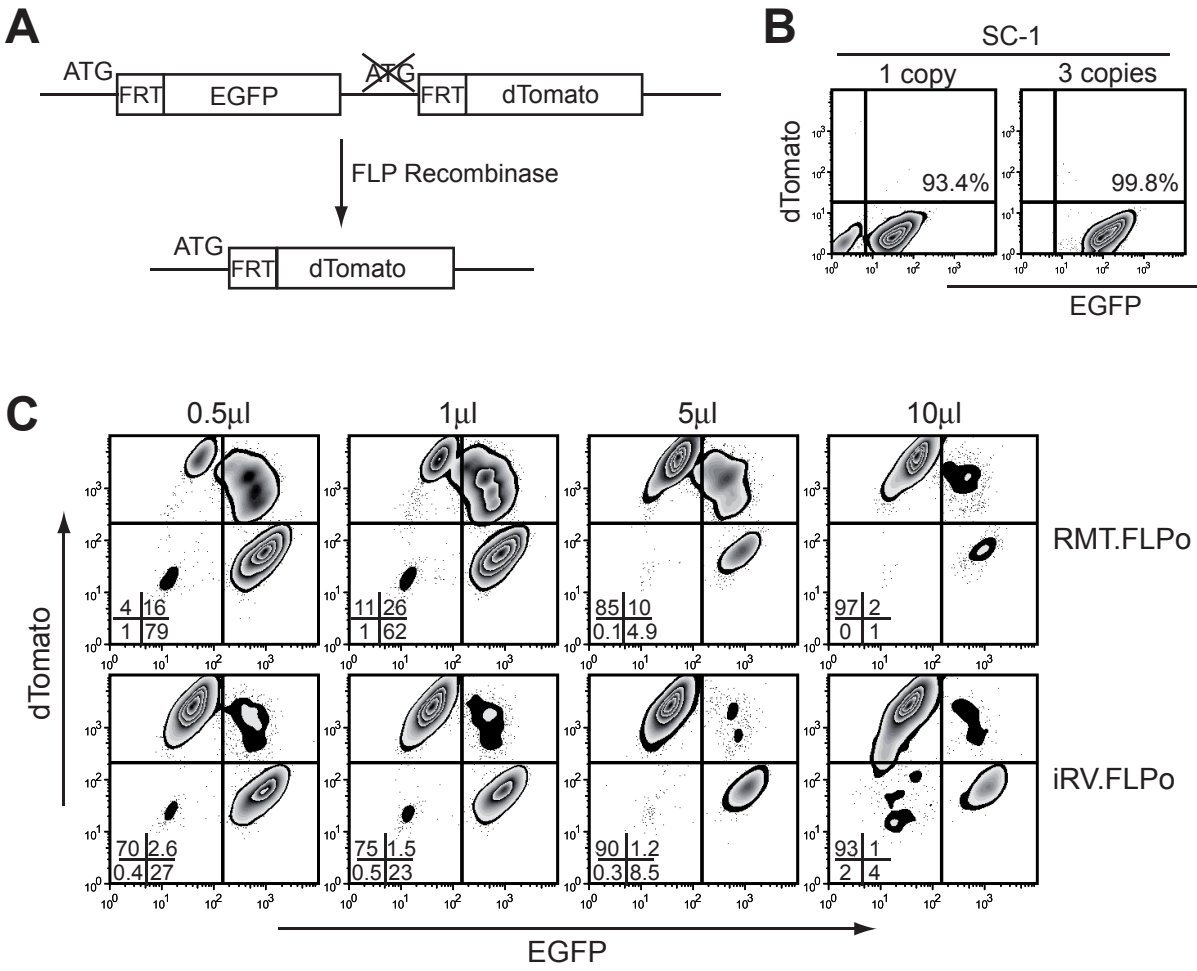

Supplementary Figure S5. Human and mouse FLP indicator cells and their FLP-dependent conversion from green to red fluorescence. (**A**) Scheme of the FLP indicator cassette as previously described (21). The EGFP gene is flanked by FRT sites and is excised after FLP recombinase exposure, which then leads to the expression of the further downstream located red fluorescent dTomato gene. (**B**) Human and mouse FLP indicator clones used in this study. Human HT1080 or mouse SC-1 fibroblasts were transduced at low MOIs with lentiviral vector particles encoding for the FLP indicator cassette. After transduction limiting dilution of the bulk population was performed (0.8 cells / well) and the total copy number of single cell clones was determined by Southern blot and quantitative PCR. The respective copy number for each FLP reporter population is shown on top of the displayed plots. (**C**) Titration of retroviral mRNA transfer (RMT) and integrating retroviral vectors (iRV) encoding for FLPo. SC-1 FLP reporter cells harboring 3 copies of the FLP indicator cassette were transduced with equal amounts of RMT.FLPo (RSF91aPBS+PRE) or iRV.FLPo (RSF91+PRE) supernatants. FACS analysis was performed two days post transduction. The dTomato+ / EGFP+ populations in the upper right quadrants reflect cells in which just 1-2 indicator alleles were recombined. In contrast, the upper left quadrants show dTomato single positive cells in which all indicator alleles were recombined (21).

Galla et al. 2011

Supplementary Figure S6

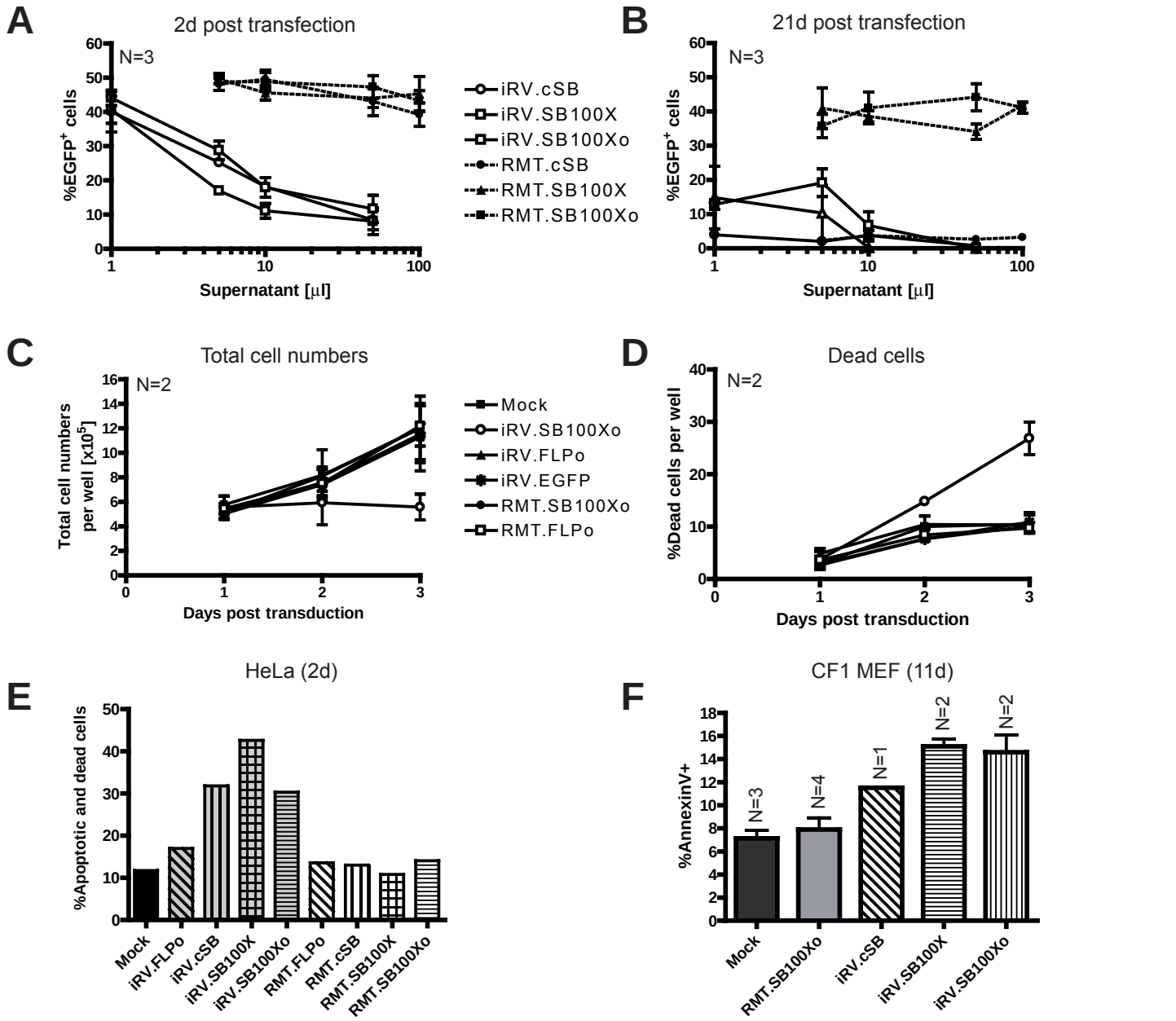

Supplementary Figure S6. Constitutive SB expression shows cytotoxicity in HeLa cells. (**A**)-(**B**) Reduced transfection / transposition rates in cells treated with iRV-based SB transposase vectors. HeLa cells were transduced with different amounts or iRV- or RMT-based vector (RSF91+PRE) supernatants and the following day transfected with transposable element plasmid harboring the EGFP expression cassette. Two and 21 days post transfection cells were analyzed for EGFP expressing cells via flow cytometry. For each graph three independent experiments are shown. (**C**)-(**D**) Trypanblue staining of HeLa cells stably expressing SB100Xo reveals inhibition of cell proliferation and increasing cell death in the first days of transduction. Cells were transduced with integrating (RSF91+PRE) SB100Xo, FLPo or EGFP or RT-deficient RMT SB100Xo or FLPo (RSF91aPBS+ PRE) particles and stained at 1 d, 2 d and 3 d post transduction for viable cells. The graphs display either the total number of cells (C) or the percentage of dead cells per culture (D). Two independent experiments were performed. (**E**) Stable expression of SB transposase induces apoptosis in HeLa cells. Graphical display of FACS plots shown in Figure 6A. The total amount of early apoptotic and late apoptotic / dead cells for integrating (iRV) and RT-deficient RMT FLPo, cSB, SB100X and SB100Xo vectors at day 2 post transduction is displayed. (**F**) Enhanced AnnexinV staining in CF1 MEFs stably expressing either type of SB transposase. CF1 MEFs were transduced with 50 µl of concentrated iRV vector particles encoding either for cSB, SB100X or SB100Xo (all RSF91+PRE). Eleven days post transduction, cells were stained with AnnexinV and analyzed via flow cytometry. Untreated Mock cells and cells treated with 3x more RMT.SB100Xo (RSF91+PRE) supernatant (150 µl) served as control. Since cells constitutively expressing SB transposase suffer from cell death and proliferation inhibition, just 2,000 events could be acquired for samples that were transduced with iRV particles (Mock and RMT.SB100Xo = 10,000 events). The corresponding numbers of replicates for each group are depicted on top of each column.

Galla et al. 2011

Supplementary Figure S7

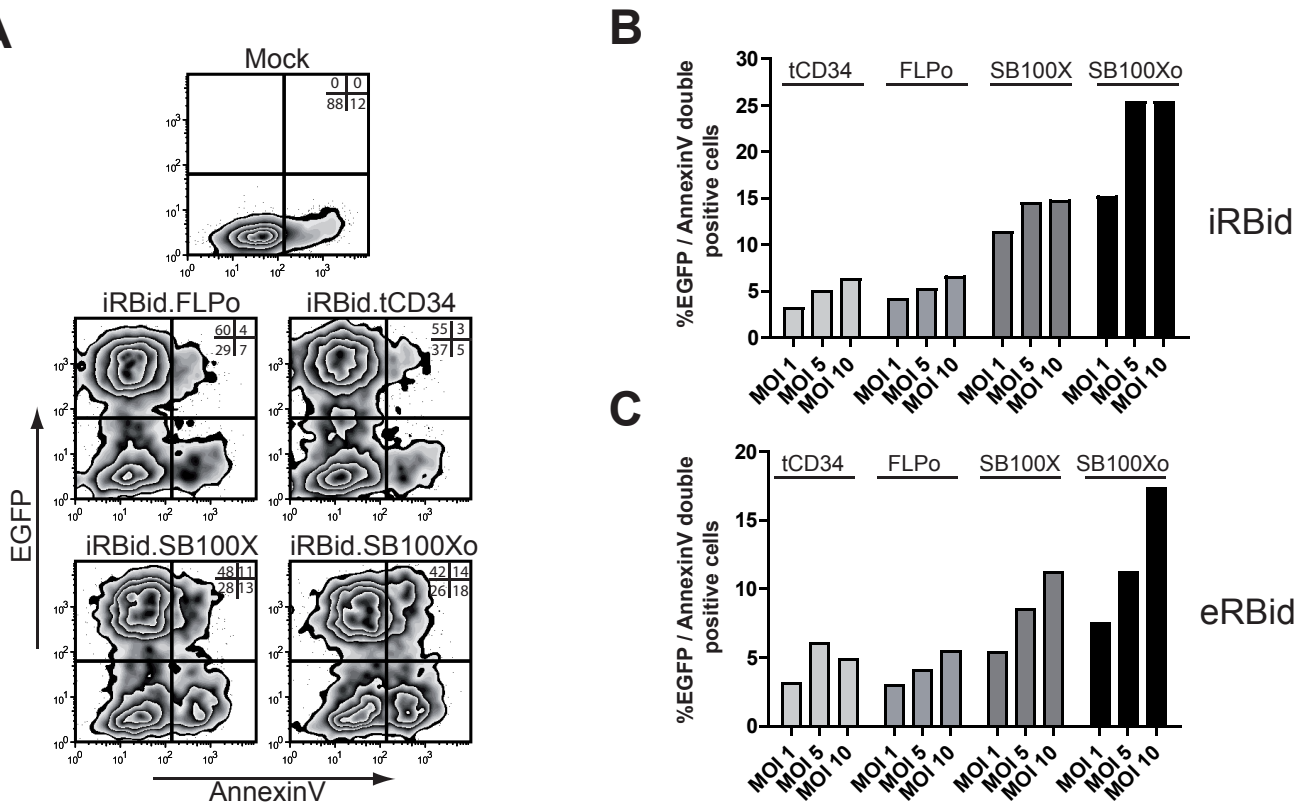

Supplementary Figure S7. Cytotoxicity of SB transposase is dose dependent. (**A**)-(**C**) HeLa cells were transduced with increasing MOIs of integrating (A and B) and episomal integrase-deficient (C) bidirectional retroviral vectors expressing EGFP together with either SB100X or SB100Xo (see Supplementary Figure S2). Four days post transduction cells were harvested and costained with propidium iodide and AnnexinV for the appearance of apoptotic and dead cells. Integrating and episomal bidirectional vectors expressing either a truncated version of the CD34 receptor (tCD34) or FLPo served as controls. In (A) representative FACS plots of cells transduced with integrating RBid vectors (MOI 1) are shown. Samples that were transduced with integrating RBid.SB100X and RBid.SB100Xo exhibit an increase of the EGFP- / AnnexinV+ cell fraction. Costaining with propidium iodide revealed that this cell fraction corresponds to late apoptotic / dead cells (data not shown).

Galla et al. 2011

Supplementary Figure S8

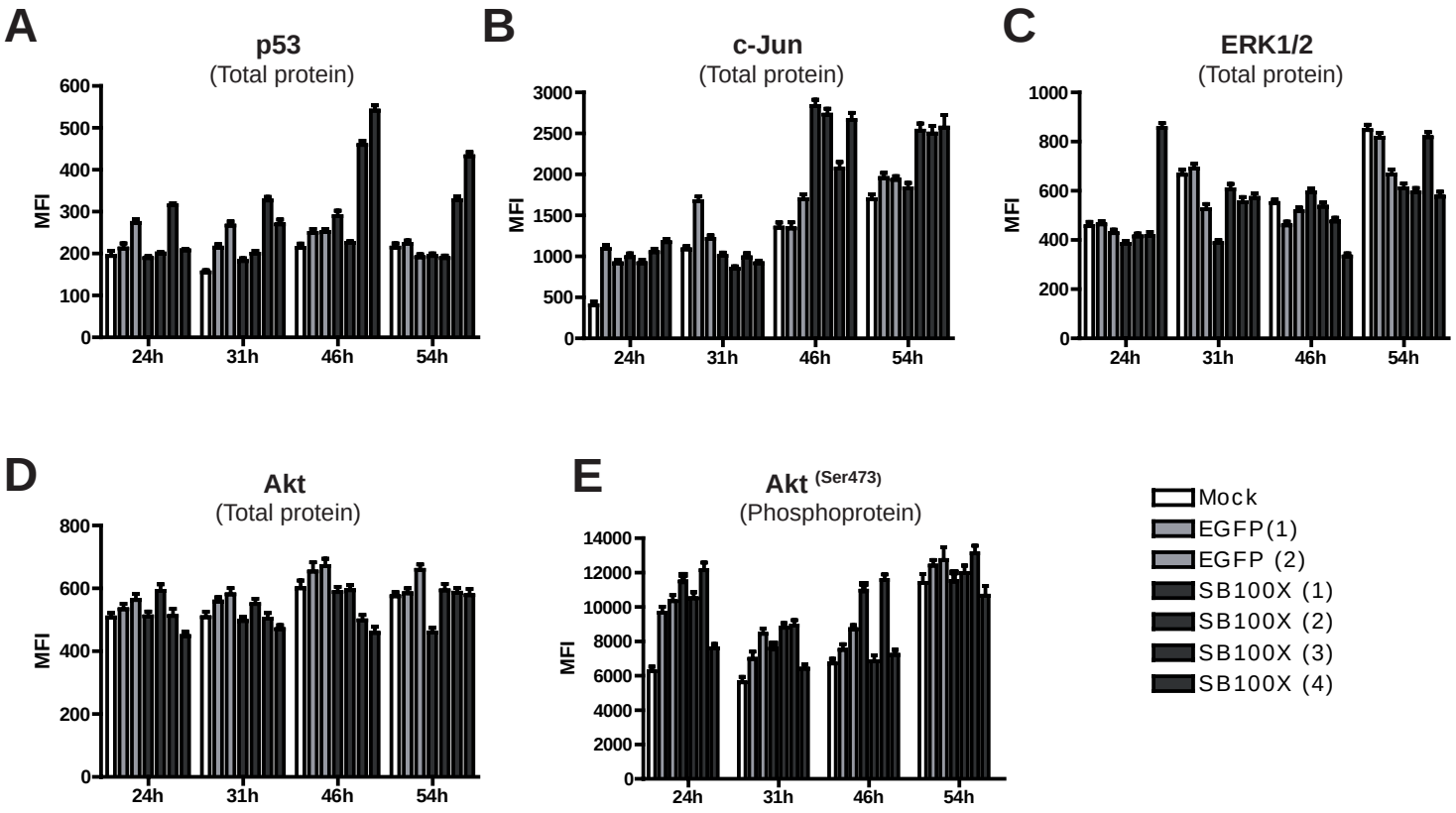

Supplementary Figure S8. Phosphoplex analysis of HeLa cells ectopically expressing SB100X or EGFP. HeLa cells were independently transduced with four different preparations (dark gray bars) of integrating iRV.SB100X (RSF91+PRE) or two preparations of corresponding integrating iRV.EGFP (light gray bars) supernatant, harvested at the depicted time points and subjected to phosphoplex analysis (see Supplementary Methods for details). Untreated HeLa cells served as mock control (white bar). Four different signalling molecules (p53, c-Jun, Akt and ERK1/2) were analyzed. (**A**-**C**) The graphs depict total p53, c-Jun and ERK1/2 protein levels for each sample as median fluorescence intensity (MFI). The corresponding phosphoprotein levels are shown in Figure 6 D-F within the main manuscript. (**D**-**E**) Total Akt protein levels (D) and its corresponding phosphorylation status (E). The error bars of all graphs depicted show the standard deviation of the mean.

Galla et al. 2011

Supplementary Figure S9

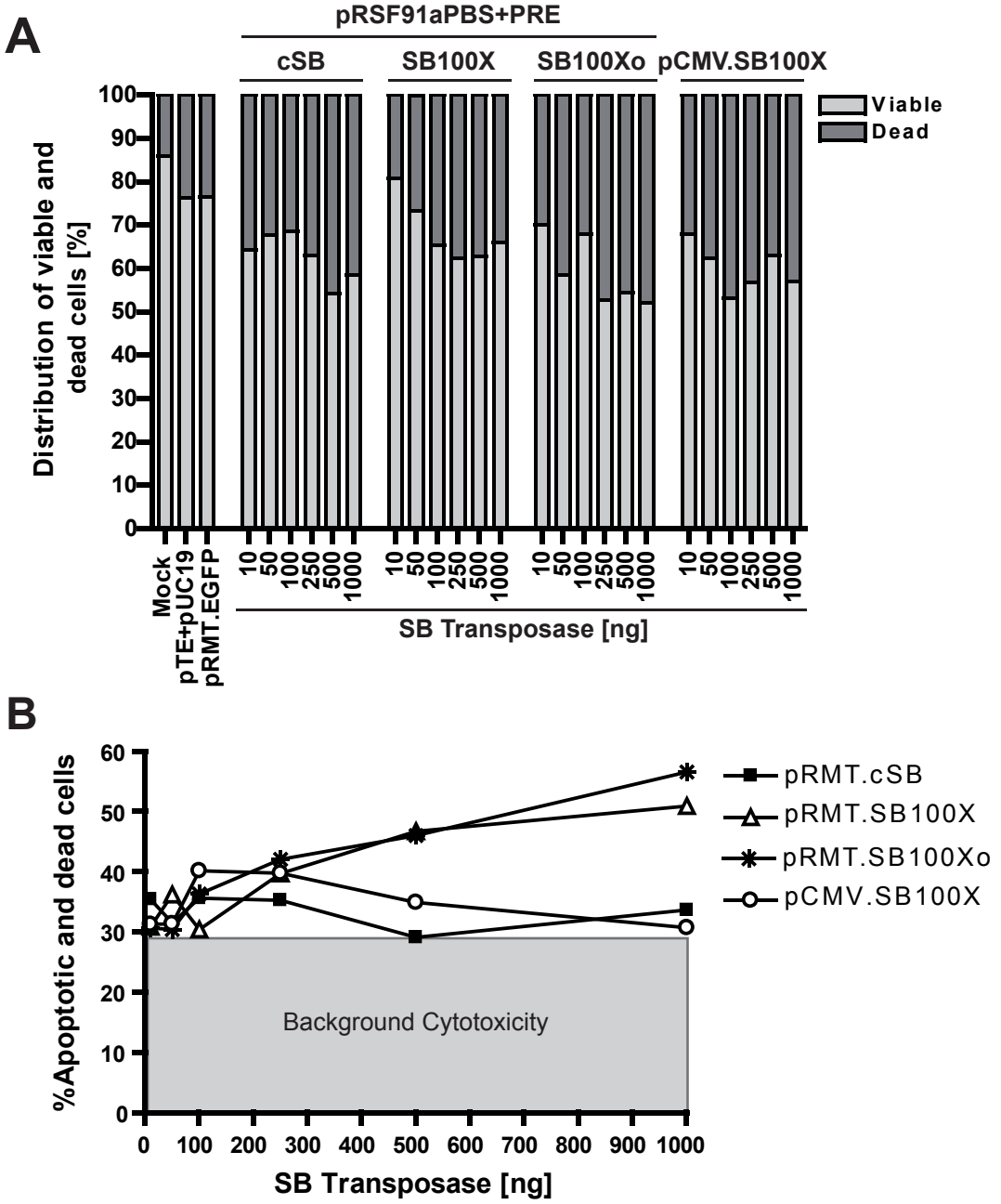

Supplementary Figure S9. SB transposase expression from transfected plasmids increases apoptosis and cell death in HeLa cells. (**A**) Distribution of viable and dead cells in cultures that were transfected with SB transposase expression plasmids. HeLa cells were transfected with 600 ng TE plasmid DNA (pTE, pSK.IR.SF.EGFP.pA.IR) and increasing amounts of nonviral (pCMV.SB100X) and gammaretroviral RMT-based (pRSF91aPBS.cSB.PRE, pRSF91 aPBS.SB100X.PRE and pRSF91aPBS.SB100Xo.PRE) SB transposase expression plasmids. Differences in plasmid quantity were adjusted with pUC19 DNA, resulting in 1600 ng transfected plasmid DNA per well. Four days post transfection cells were harvested, stained with trypan blue and analyzed for cell viability. Non-treated mock cells and cells that were transfected with pTE+pUC19 only (600 ng + 1000 ng, respectively) or with 2 µg of a gammaretroviral RMT-based EGFP expression plasmid (pRMT.EGFP (19)) served as controls. (**B**) Increased occurrence of apoptotic and dead cells in cultures that were transfected with SB transposase expression plasmids. Cell cultures depicted in (A) were co-stained with AnnexinV and propidium iodide (PI) and analyzed via flow cytometry. The graph displays the proportion of EGFP, AnnexinV and PI positive cells within these cultures. The "background cytotoxicity" comprises normal occurrence of apoptotic and dead cells within a culture as well as the PEI transfection-induced cytotoxicity (see also the three left bars in (A)). Interestingly, pRMT.cSB and pCMV.SB100X showed maximum apoptotic and dead cell levels at concentration 100 ng and 250 ng rather than at higher concentrations. The resulting inconsistency to the corresponding trypan blue data shown in (A) might be due to several washing steps during the staining procedure where damaged / dead cells got probably removed.